Collision-Induced Dissociation by Helium: A Piecewise Construction of the Cross Section

L. Poisson, P. de Pujo, V. Brenner, A.-L. Derepas, J.-P. Dognon, and J.-M. Mestdagh*

Laboratoire Francis Perrin (CNRS FRE-2298), CEA/DRECAM/Service des Photons, Atomes et Molécules, C.E. Saclay, F-91191 Gif-sur-Yvette Cedex, France

Received: August 1, 2001; In Final Form: November 15, 2001

Molecular dynamics calculations were performed to simulate the collisions between a helium atom and either a water dimer or various geometries of the $Na(H_2O)_3^+$ cluster. The trajectory calculations were interrogated to document the partial conversion of the collision energy into internal excitation of the cluster. Owing to the small size of helium, the collision energy, which is transferred as an impulse to the cluster, is deposited initially on one of the atoms of the cluster. The amount of transferred energy in the atom that is collided depends of its mass, and more interestingly if it is involved in a H-bond like bonding with a water molecule. The general rules that have been drawn to describe the energy transfer allowed us for a picewise construction of collision-induced-dissociation cross sections, each piece being the energy tranferred toward a specific atom of the cluster. This offers a framework for extracting quantitative information on binding energies from collision-induced-dissociation experiments by helium in $M(H_2O)_n^+$ systems (M is a metal atom). Importantly, the fit to the experimental data that is allowed by the present model is not restricted to the threshold energy region of the CID cross section. An application is given for the He + $Au(H_2O)_{1,2}^+$ collision.

1. Introduction

Collision-induced-dissociation (CID) is a well-established technique to inform on the structure and energetics of molecular ions and ionic clusters.[1] Two recent reviews cover the subject.[2,3] A heavy projectile, Xe, is commonly used to run such experiments when quantitative thermochemistry is the main purpose.[3] With this projectile indeed, all the collision energy (almost exclusively the ion kinetic energy in most experiments) is transferred into the ionic target as vibrational excitation and the dissociation proceeds through an evaporation process. At threshold, the dissociation products are left essentially at 0 K, thus providing an accurate information on binding energies. Fancy data analysis techniques, including corrections to account for the time window of the experiments, are needed to give the full power to the method.[3−6]

Lighter rare gas projectiles, such as neon or argon, can also be used in CID experiments. For example, a CID study of VO^+ has shown that with neon as projectile, the increase of the CID cross section at threshold is too slow to bring a useful information on the V^+−O binding energy.[7] The poor efficiency of light gases as CID projectiles on heavy targets has also been observed on the theoretical side.[8,9] This is easy to rationalize with the help of impulsive models based on classical mechanics. The collision of a light projectile with a target formed of heavy atoms is indeed essentially elastic and transfers almost no collision energy as internal excitation of the target.[10−12] This point has been exemplified a number of times in calculations where projectile of various masses, Ne, Ar, and Xe are collided with targets such as Al_6 and Al_{13}.[13,14] Nevertheless, studies exist, where the lightest rare gas, helium, is used as a projectile in CID experiments. For example, both experimental and theoretical studies have been performed in the group of Barat and Fayeton on Na_n^+ + He collisions at fairly large collision energies (100 eV). Three different dissociation mechanisms have been found in this case:[15−18] (i) a direct impulsive mechanism (IM1) where both the energy deposition and the dissociation are impulsive; (ii) a two step impulsive mechanism (IM2) where the energy is deposited impulsively into the cluster, but the dissociation which follows is an evaporation; and (iii) an electronic mechanism involving electronically excited levels of the cluster (EM). In this classification, impulsive energy deposition is indicated by opposition with the formation of a long-lived complex.

More recently, helium has been used as a projectile in a CID experiment to probe the energetics of $Fe(H_2O)_2^+$, $Co(H_2O)_2^+$, and $Au(H_2O)_2^+$ cluster ions produced in a supersonic expansion.[19,20] These works have shown that two isomers of these ions exist in the beam. One has both water molecules directly attached to the core metal ion (first solvation shell water). In the other, one of the water molecules is not directly bonded to the metal and is located in the second solvation shell.[20] There are two reasons for the light helium projectile to be able in this case to transfer enough energy into the cluster ions to induce its dissociation and to bring meaningful information on its energetics: (i) helium has a small size and (ii) the cluster ion target contains atoms of very different masses, H (1 amu), O (16 amu), and either Fe (55 amu), Co (59 amu), or Au (197 amu). Hence, in an impulse picture of the He/target collision, helium collides only one atom in the subunits forming the cluster. Such a localized energy deposition has already be encountered in the somehow different context of He + Ar_n collisions.[21] The important point in He + $M(H_2O)_n^+$ collisions is that the energy transfer is optimum when the mass of the helium projectile matches that of the atom which has been collided. With this mechanism in mind, we therefore anticipate that the initial deposition of the energy into the cluster is very inhomogeneous.

The present work aims at bringing some light into the energy transfer in $M(H_2O)_n^+$ + He collisions (M is a metal atom). More precisely, it explores the possibility of a piecewise contruction of the energy transfer, each piece being the atom that is collided

* To whom correspondence should be addressed. FAX: 33-1-69 08 84 46. E-mail: jmm@drecam.saclay.cea.fr.

10.1021/jp012964y CCC: $22.00
Published on Web 02/12/2002

by helium, with the aim of interpreting quantitatively CID experiments performed on $M(H_2O)_n^+ + He$ systems.

For this purpose, molecular dynamics simulations were performed on relevant models of the above-mentioned $He + M(H_2O)_n^+$ collisions, which address specifically the question energy transfer into a composite system. Of course, high quality potentials which well reproduces the structure of the water molecules have been used in the calculation. Two different targets have been considered. First, the most stable geometry of the water dimer $(H_2O)_2$ was investigated as a benchmark of our approach. Second, three different geometries of the $Na(H_2O)_3^+$ cluster ion were considered as a representative model of $M(H_2O)_n^+$. By the way, the effect of the cluster geometry in the He−Cluster energy transfer has been examined. These results are further used to predict the energy dependence of CID cross sections, in $He + Na(H_2O)_3^+$ collisions and more generally in $He + M(H_2O)_n^+$ collisions, where M is a metal, hence giving the framework to extract a quantitative information from CID measurements with helium. An application is given for the $He + Au(H_2O)_2^+$ system where detailed experimental data on CID are available.[20] High quality ab initio calculation were performed on $Au(H_2O)_2^+$ in order to check the reliability of the information provided by analysis of the CID data.

As a side result, the present work allows to better understand the fragmentation mechanism that follows the energy transfer.

2. Simulation Method

The $He + M(H_2O)_n^+$ collision is modelized by classical dynamics using a molecular dynamics program. The use of classical mechanics rather than quantal is justified by the large energy transfers that are to be considered in the present work. We are concerned indeed with collision-induced dissociation. Hence, the only energy transfers toward the cluster that are relevant here are those exceeding the binding energy of, at least, one water molecule of the cluster. Such energy transfers are large compared to the vibrational constant of the weak vibrational modes that are excited by collision with helium, thus justifying classical mechanics. As we shall see, the use of classical mechanics leads to a series of simplifications such as neglecting the zero-point energy and the internal energy of the cluster before collision.

We first describe rapidly the molecular dynamics program and the way the simulations are conducted. Then we report in more detail the model potential used to describe realistically the interaction energy between the subunits forming the clusters. Finally we describe rapidly the initial structures of the clusters before collision with helium.

2.1. The Molecular Dynamics Program and the Trajectory Sampling. *The Molecular Dynamics Program.* The program has been described extensively in former works.[21−23] It has been optimized to treat of the dynamics of weak cluster modes, disregarding the hard modes corresponding to the deformations of the molecular subunits forming the cluster. In the present case, this corresponds to keep the water molecules as rigid. The integration algorithms are that of Verlet[24] for the translations and that of Fincham[25] for the molecular rotations.

Input Parameters. Steps of 0.5 fs are used to integrate the movement equations. This ensures a stability of the energy always better than 0.05% over a full trajectory calculation. Trajectory calculations are started at distances larger than 10 Å for $He + (H_2O)_2$ and larger than 12 Å for $He + Na(H_2O)_3^+$: these distances depend on the trajectory that is sampled (see below). The trajectories are followed respectively for 480 and 900 fs. With this choice, helium is far enough from the cluster at the end of the calculation such that it does not interact with the cluster any more.

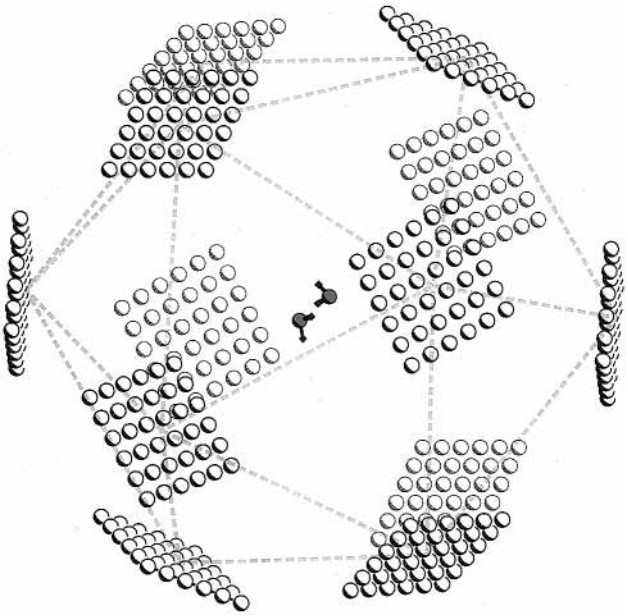

Figure 1. Sampling scheme of the trajectories on each face of a dodecahedral surrounding the cluster which is to be collided (a water dimer in the figure). Each circle indicates the starting position of a different trajectory.

Initial Temperature. Molecular dynamics calculations involving clusters could be performed by fixing an initial temperature to the cluster that corresponds to an experimentally determined one.[21−23] In that case a statistical averaging over thermal deformations of the cluster is needed. We shall see in section 5 when calculating CID cross sections that only large energy transfers toward the cluster are relevant here, especially because the behavior of the cross sections substantially above the CID threshold is the most important. As a result, effects associated with the internal energy contained by the cluster can be neglected. Hence calculations have been performed for a 0 K initial temperature of the cluster, the trajectories being sampled as explained in next paragraph in order to account for the various impact geometries of helium with the cluster.

Trajectory Sampling. The calculations are performed in a reference frame where the 0 K cluster is at rest before collision and located at the origin of the reference frame.

The sampling procedure is schemed in Figure 1. Each helium trajectory is initiated as starting from one of the 12 faces of a dodecahedral whose center is the origin of the reference frame. The direction of the initial velocity of helium is perpendicular to the face from where the trajectory is starting. The starting position of the trajectory on each face is regularly sampled by increment of 0.25 Å. By the way, each trajectory amounts for a cross section of $0.25 \times 0.25/12 = 5.2 \times 10^{-3}$ Å^2. This will be used when using the trajectory calculations to calculate CID cross sections.

A dodecahedral has no symmetry element in common with the cluster that is to be collided. Hence, an initial spatial orientation of the cluster can be chosen, so as no symmetry axis of the cluster coincides with a symmetry axis of the dodecahedral. By the way, the set of trajectories that was calculated fully samples impact directions and impact parameters on the cluster. The sampling on the impact parameter is provided by the various starting points on each face of the dodecahedral, where the sampling on the impact direction is provided by the twelve faces of the dodecahedral.

The distance between the center of the dodecahedral and each of its faces determines the closest starting distance between helium and the cluster, respectively chosen as 10 Å and 12 Å for $He-(H_2O)_2$ and $He-Na(H_2O)_3^+$ as said above. The trajectory sampling corresponds to calculating 6912 and 20172 trajectories to simulate the $He+ (H_2O)_2$ and $He+Na(H_2O)_3^+$ collisions, respectively.

Collision Energy. A values of 5000 m s^{-1} was chosen for the initial velocity of helium colliding the water dimer. This corresponds to a center of mass collision energy of 0.47 eV. A collision energy of 1.26 eV was examined for $Na(H_2O)_3^+$. It corresponds to a 8000 m s^{-1} initial velocity of helium. We shall see the reason for exploring a single collision energy in section 4.2.

2.2. Interaction Potential. A right choice of the intermolecular potential shows up as providing realistic predictions of the initial cluster geometry. Of course, it is the necessary condition to get reliable predictions in the molecular dynamics calculations. For this reason, the interaction potential used in the present work is described in some details.

We have used a model potential that has been initially proposed by Claverie et al.[26,27] It has been reexamined first by Brenner et al.[28,29] and more recently by Derepas et al.[30] It includes all the important contributions to the interaction energy: electrostatic, polarization, repulsion, and dispersion. Each contribution is expressed by an analytical formula which derives from its expression at the second order in the exchange perturbation treatment of the interaction. It has been chosen to give a reliable description of the corresponding interaction at all intermolecular distances.[26,27]

Model Potential. We first examine the general construction of the potential, then we shall see how it is applied for modelizing the $(H_2O)_2$ and $Na(H_2O)_3^+$ clusters.

The potential energy surfaces are expressed in terms of the $6(n - 1) + 3m$ intermolecular degree of freedom where n is the number of water molecules of the system and m the number of metal ions ($m = 0$ or 1). The molecules are frozen at their equilibrium geometry and are described by six coordinates, three coordinates for the rotation (Euler angles) and three other for the translation.

The electrostatic term treats of the interaction between all the permanent multipoles. Its expression is therefore a straightforward summation of multipole-multipole interaction terms.

Polarization is inherently a *n*-body term which can be calculated according to one of the following two approaches.

The first approach is approximate but efficient in terms of calculation time.[26−29] It treats the total polarization energy as the sum of the polarization energy of each molecule forming the cluster in the field created by the permanent multipoles of all the cluster constituents. Only dipolar polarizabilities of each molecular subunit are considered, theses dipolar polarizabilities being derived from mean bond experimental polarizabilities. Such an approach accounts for the most important *n*-body terms, but contributions of high order such as polarization via quadrupole polarizability, hyperpolarization, or back polarization (induced moments polarizing neighboring molecules) are neglected.

In the second approach, the description of the polarization term is improved by taking into account the correction to the electric fields resulting from the induced dipoles.[30]

In the calculation of the electrostatic-polarization terms, the multipole distribution of each molecular subunit is generated from the multipolar multicentric development of the electronic distribution through a systematic procedure of reduction of the number of centers.[31] The multipole distribution of each molecular subunit is described by sets charge + dipole + quadrupole located on each atom and on one point per chemical bond. The multipolar multicentric development is derived from the wave function obtained via an ab initio calculation. An extended basis set and the electronic intramolecular correlation have to be introduced in the calculation in order to describe accurately the electrostatic interactions and the corresponding electric fields.[28,29]

The repulsion and dispersion terms are the sums of atom−atom contributions. Repulsion takes into account the variation of the electronic population of each atom in the molecules and its influence on the van der Waals radius. The dispersion terms include contributions up to C_{10}/R^{10} as well as an exchange contribution.

The recent developments of the model potential introduce additional atomic parameters in the dispersion−repulsion terms in order to allow for the description of cations such as sodium, i.e., cations which do not lead to a significant charge transfer toward the molecular environments. Furthermore, some atomic parameter of atoms in molecules have been readjusted. A full account of this is given in ref 30.

In the Present Case. The multipole distribution of the water molecule is obtained at the second-order Moller−Plesset perturbation (MP2) level of theory using a large basis set built on the primitive sets of van Duijneveldt[32] contracted to obtain basis set of quadruple-ζ quality (O, 14s7p/8s4p; and for H, 10s/4s) and augmented by two sets of polarization functions (sets of polarization functions: O(1.5, 0.35) and H(1.4, 0.25). We then obtain a good agreement between the calculated and experimental permanent dipole moment of the molecule. For the sodium cation, the multipole distribution consists of a charge of +1 ua and the polarizability is the experimental one. Furthermore, the atomic parameters of the sodium cation and the water molecule atoms, required in the calculation of the dispersion−repulsion terms, have been derived from sophisticated ab initio calculations performed on the $(H_2O)_2$ and Na systems according to the strategy developed by Derepas et al.[30]

The second approach mentioned above for calculating the polarization term is very time-consuming in the calculations. Hence, the first approach was used. Of course we have checked that doing so, does not introduce dramatic distortions in both the geometry and energetics of the clusters $(H_2O)_2$ and $Na(H_2O)_3^+$ considered here. [This would not have been the case for $Na(H_2O)_2^+$. Two equilibrium structures ($(H_2O)Na^+(H_2O)$ and $Na^+(H_2O)(H_2O)$) are predicted by the second approach, whereas only one appears when using the approximate first approach. The existence of two isomers is further confirmed by ab initio calculation.[30]] The geometry of the water dimer is the same along both approaches, within 10^{-2} Å for distances and 0.2° for angles and is close to that available from other theoretical works.[33,34] The strength of the H-bond is also comparable in both approaches and is close to that found experimentally (0.23 ± 0.03 eV,[35] 0.23 ± 0.01 eV[36]). When turning to the three isomers of the $Na(H_2O)_3^+$ cluster ions considered here, both approaches lead to almost identical energies and structures for the two most stable isomers. The energetics of the third isomer is close also (see Table 2 in the next section), but not the geometry. The second shell water molecule is farther away from the other water molecule in the simplified approach. This is not believed to cause troubles for the purpose of the present work.

2.3. Equilibrium Structures. The procedure developed by Bertolus et al.[37] is used to determine equilibrium structures. It can be resolved into three steps: (i) a global exploration of the

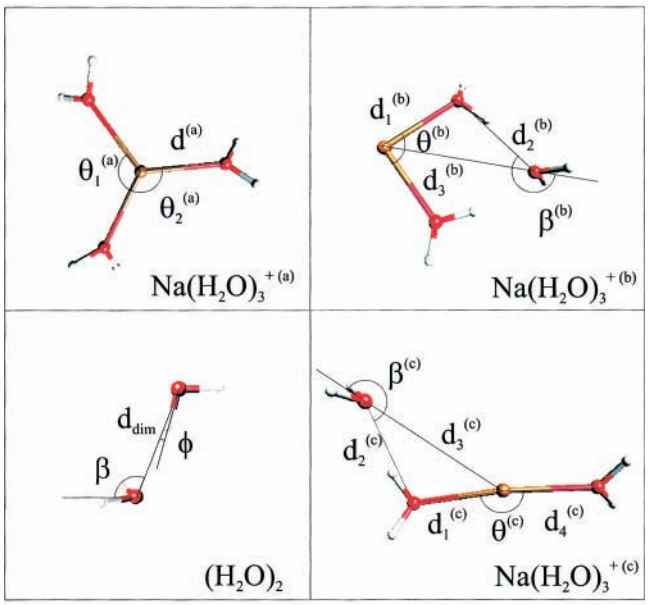

Figure 2. Structure of the clusters before collision with helium. The values of the angles and distances that label each structure are given in Table 1. The geometry of the water dimer and that of the isomer (a) of $Na(H_2O)_3^+$ are associated with global minima of the corresponding potential energy surface. The other two isomers of $Na(H_2O)_3^+$ correspond to secondary minima.

potential energy surface is performed using the Monte Carlo growth method, (ii) the isomer conformations obtained from this exploration are sorted out, (iii) each isomer geometry is optimized by a local minimization method and the existence of each minimum on the potential energy surface is proved by calculating the Hessian.

The structure found for the water dimer $(H_2O)_2$ and for the three most stable isomers of the $Na(H_2O)_3^+$ clusters are shown in Figure 2. The angles and distance defining the structure quantitatively are given in Table 1. The calculated energetics of these ions are given in Table 2. As said above, both the binding energy and the geometry found for the water dimer are close to that available in the literature.[33−36]

A guideline should be drawn at this point. Strictly speaking, an H-bond is the intermolecular bond in the water dimer. When considering the $Na(H_2O)_3^+$ clusters hereafter, we will see that the energetics of the bond between a water molecule in the second solvation shell and the remaining of the cluster deviates both in energy and geometry from a pure H-bond. A substantial contribution of the metal ion core is superimposed to the interaction energy between the second shell water molecule and the first shell one that is bonded to it. Hence, the bond between two such water molecules deviates from the above definition of a H-bond. Nevertheless, by convenience, we still call it a "H-bond", but with quotation marks to stress the difference.

The most stable isomer of $Na(H_2O)_3^+$ has the three water molecule in the first solvation shell. It has a C_2 symmetry, little perturbed from the higher D_3 symmetry. The hydrogen atoms are disposed so has the cluster resembles an helix. The calculated adiabatic binding energy of one water molecule in this isomer, 0.74 eV, is in excellent agreement with the value experimentally determined in the group of Armentrout, 0.72 ± 0.06 eV.[38]

The second isomer of $Na(H_2O)_3^+$ (isomer (b) in Tables 1 and 2 and in Figure 2), has a water molecule in the second solvation shell, which is bonded to the two others by an "H-bond". This isomer belongs to the C_2 symmetry group. The $\theta^{(b)}{}_1$ angle of this structure is smaller than the corresponding angles $\theta^{(a)}{}_{1 \text{ or } 2}$ in the most stable isomer, 94° versus 118° and 121°. This indicates that the presence of the second shell water molecule reduces the effect of repulsion between the remaining first shell water molecules. The sum of pairwise interactions (without polarization) between the second shell water molecule and the directly bonded water molecule leads to an attractive binding of 0.12 eV (0.18 eV in the water dimer), whereas the binding to the ionic core amount to 0.35 eV and corresponds to only electrostatic interaction. This indicates clearly that the bond involved in this case is not a true H-bond. This can be observed also when considering the angle $\beta^{(b)}$, which is very different from the corresponding angle in the water dimer, 216° versus 106.2°.

The last isomer that is considered for $Na(H_2O)_3^+$, isomer (c), has one water molecule in the second solvation shell, but in contrast with isomer (b), it is involved in only one "H-bond". This isomer has therefore a filament structure. The contribution of pairwise interactions in the energetic of the "H-bond" is 0.093 eV with the other water molecule and 0.35 eV with the cation. Again, the binding of the H_2O molecule is not a pure H-bond. As well, the angle $\beta^{(c)}$ has a different value from that found for the equivalent angle in the water dimer.

3. Ab initio Calculation on the $Au(H_2O)_{1,2}^+$ Cluster Ions:

These calculation were performed to test the procedure used in section 5.2 for analyzing CID data and getting quantitative information on both the structure and the binding energy of the $Au(H_2O)_{1,2}^+$ cluster ions.

The calculations were conducted in two steps. First, full geometry optimizations have been performed at the MP2 level of theory and then harmonic frequencies of the optimized geometries have been calculated at this level in order to both characterize the obtained stationary points and determine the zero-point energies (ZPE). Second, single-point energy calculations at the coupled cluster theory with perturbative triples (CCSD(T)) have been performed on the MP2 optimized geometries.

For the water molecule, we used the basis set described in section 2.2. For the gold atom, as heavy elements exhibit relativistic effects which have significant influence on physicochemical properties such as ionization potential, we used the averaged relativistic effective core potential (RECP) developed by Roos et al.[39] (60e-, $[Kr]4d^{10}4f^{14}$ core) and the original associated basis sets were augmented by additional one p diffuse (0.0504) and two f polarization functions (0.8204, 0.1940) resulting in a (5s6p4d2f/4s4p3d2f) basis set. We have checked that, at the MP2 level of theory, the basis sets chosen allow to reproduce correctly the experimental values of physicochemical properties of the entities involved in the system (i.e., ionization potential, polarizability, or permanent moment). The binding energies of the clusters (D_e) were computed as the difference between the energy of the entire system and the sum of those of the isolated species. Furthermore, the basis set superposition error (BSSE) was taken into account in the calculation of the D_e's and was computed in the counterpoise approximation (CP). Finally, from both the D_e values obtained at the CCSD(T)/MP2 level with BSSE and the ZPE values obtained at the MP2 level, the D_0 values were computed.

For the clusters carrying two water molecules, two starting configurations have been considered and lead to two different equilibrium structures. In the first configuration denoted afterward $(H_2O)Au(H_2O)^+$, both water molecules are in the first solvation shell. They are bonded to the gold ion directly and do not interact with each other. In the second configuration

TABLE 1: Angles and Distances Defining Quantitatively the Structures Shown in Figure 2

$(H_2O)_2$	C_s[a]	$\beta = 106.2°$, $\phi = 6.5°$, $d_{dim} = 2.88$ Å
$Na(H_2O)_3^+$ (a)	C_2 almost D_3	$\theta^{(a)}_1 = 118°$, $\theta^{(a)}_2 = 121°$, $d^{(a)} = 2.38$ Å
$Na(H_2O)_3^+$ (b)	C_2	$\theta^{(b)} = 94°$, $\beta^{(b)} = 216°$, $d^{(b)}_1 = 2.32$ Å, $d^{(b)}_2 = 2.90$ Å $d^{(b)}_3 = 3.95$ Å.
$Na(H_2O)_3^+$ (c)	C_1	$\theta^{(c)} = 173.4°$, $\beta^{(c)} = 214°$, $d^{(c)}_1 = 2.30$ Å, $d^{(c)}_2 = 2.80$ Å, $d^{(c)}_3 = 3.98$ Å $d^{(c)}_4 = 2.36$ Å

[a] The second column gives the symmetry group to which each cluster ion belongs.

TABLE 2: Energetics of the Water Dimer $(H_2O)_2$ and of the Three Isomers of $Na(H_2O)_3^+$ Labeled (a), (b), and (c) in Figure 2[a]

structure	total energy (eV)	incremental BE (eV)
$(H_2O)_2$	0.21[a]/0.22[b]	0.21[a]
$Na(H_2O)_3^+$ (a)	2.59[a]/2.55[b]	0.74[a]
$Na(H_2O)_3^+$ (b)	2.43[a]/2.42[b]	0.58[a]
$Na(H_2O)_3^+$ (c)	2.36[a]/2.38[b]	0.51[a]

[a] The second column displays the binding energy of the clusters, whereas the third column gives the incremental binding energy, given the binding energy of $Na(H_2O)_2^+$ (1.85 EV). Strictly speaking, these energies refer to D_e and ΔD_e, but correspond to dissociation energies D_0 and ΔD_0 in the perspective of a classical calculation. [c] Calculations using the refined approach (see text, section 2.2). [b] Calculations using the approximate approach for the polarization energy term.

TABLE 3: Geometrical Parameters (Bond Lengths in angstroms and Angles in Degrees) for the $Au(H_2O)_{1,2}^+$ Systems

	Au−O distance			angle		
cluster	this work	ref 42	ref 41	this work	ref 42	ref 41
$Au(H_2O)^+$ (C_s)	2.12	2.12[a] (2.14)[a]	2.13 2.16[c]	151[c]	149[c]	133[c]
$(H_2O)Au(H_2O)^+$ (C_2)	2.05	2.03[b] (2.07)[b]		141[c]		
$Au(H_2O)(H_2O)^+$ (C_s)	2.07 4.03			120.7 157.0[d]		

[a] MP2 level within basis set: RECP of Dolg (60e-, $[Kr]4d^{10}4f^{14}$ core) associated with a (8s7p5d1f/7s5p4d1f) basis set for the gold atom and the aug-ccpVDZ basis set for the others atoms. The values in parentheses correspond to the values optimized at the CCSD(T) level. [b] MP2 level within basis set: RECP of Dolg associated to a (10s8p7d1f/9s5p6d1f) basis set for the gold atom and the augmented TZ2P basis set of Dunning for others atoms (O, 10s6p2d1f/5s3p2d1f and H, 5s2p1d/3s2p1d). The values in parentheses correspond to the values partially optimized at the CCSD(T) level, i.e., only the Au−O bonds are reoptimized at this level. [c] Out-of-plane angle formed by the Au−O bond and the bisector of the two water hydrogens. [d] Au−O−O angle, angle formed by the O−O bond and the bisector of the two water hydrogens of the second water of the molecule.

denoted afterward $Au(H_2O)(H_2O)^+$, one water molecule is in the first shell and is bonded to the gold ion directly whereas the other molecule is in the second solvation shell. These structures are the somehow equivalent to structures a) and c) already seen for the $Na(H_2O)_3^+$ ions in section 2.3. The incremental quantities ΔD_e and ΔD_0 have been calculated also. The calculations have performed using the GAUSSIAN 98 package.[40]

The results are reported in Table 3 and 4. For comparison, the results obtained by Hrusák et al. for the Au system[41] as well as those of Feller et al.[42] for Au and $(H_2O)Au(H_2O)^+$ are also reported in the tables. The present calculations are in good agreement with the previous calculations when available. This give confidence on both basis set and level of theory that is used here, i.e., CCSD(T)/MP2 level corrected for BSSE within a reasonable basis set (at least RECP with a associated basis set with f functions for the gold atom and triple-ζ quality basis set for others atoms).

4. Results and Discussion of the Molecular Dynamics Calculations

4.1. Energy Transfer Mechanism. The collision duration between helium and the cluster tells whether the collision can be considered as sudden or not. Of course there is some flexibility in defining the collision time. Only collisions transferring more than 60% of the helium kinetic energy to the cluster are considered for this purpose. In this case, trajectory calculations have shown that helium spend about 34 fs within the van der Waals spheres about the $Na(H_2O)_3^+$ clusters. This duration is shorter than the shortest vibration period that is expected for the intermolecular deformation modes of the clusters: 66 fs for a mode of 500 cm^{-1} energy. Hence the subunits forming the cluster do not have time to move during the collision. As a result, the collision can be considered as sudden and the energy transfer to weak modes is essentially impulsive. This fits with the standard picture where CID is described as a two-step process.[2] We discuss this question further in section 6.

4.2. Histograms of Energy Transfer. From above, we know that the cluster has no time to move internally during the collision with helium (remember that only the weak modes of the cluster are taken into consideration in the present work). As a result, the cluster behaves as a "wall", against which helium rebounds. Hence the helium trajectory remains the same whatever the collision energy. Of course, the impulse given to the "wall" changes as the collision energy is changed. It is proportional to the relative impulse of helium with the cluster. Hence the energy transferred into the cluster is simply a fraction of the collision energy. This justifies that calculations are performed at a single collision energy. [We have checked this statement numerically by running calculations on $He + (H_2O)_2$ collisions at 0.92 eV. The percentage of energy transferred to the cluster at this energy is quantitatively comparable to that presented in the present section at 0.47 eV collision energy.] Of course the fraction of energy transferred into the cluster changes from one trajectory to the other. As a result, the relevant property provided by the calculations when sampling trajectories is an histogram giving the number of trajectories responsible for transferring a given fraction of the collision energy into the cluster.

This consideration can be refined further when considering both the impulse character of the collision and the small size of helium. It is indeed worthwhile to interrogate each calculated trajectory in order to determine which atom of the cluster has been collided by helium. The criterion that was chosen for such a propose is to assign the collision with helium to the atom which had the closest approach with helium during the collision. This assignment is questionable in three cases: (i) when helium rebounds several times in the cluster; (ii) when helium collides a bond just between two atoms; (iii) for collisions at large impact parameters, when helium is flying at quite large distances from the cluster, the assignment is ambiguous. Many trajectories correspond to the later situation but they are not associated with a significant energy transfer. For this reason the effect of this ambiguity is not very important as long as significant energy transfers are considered.

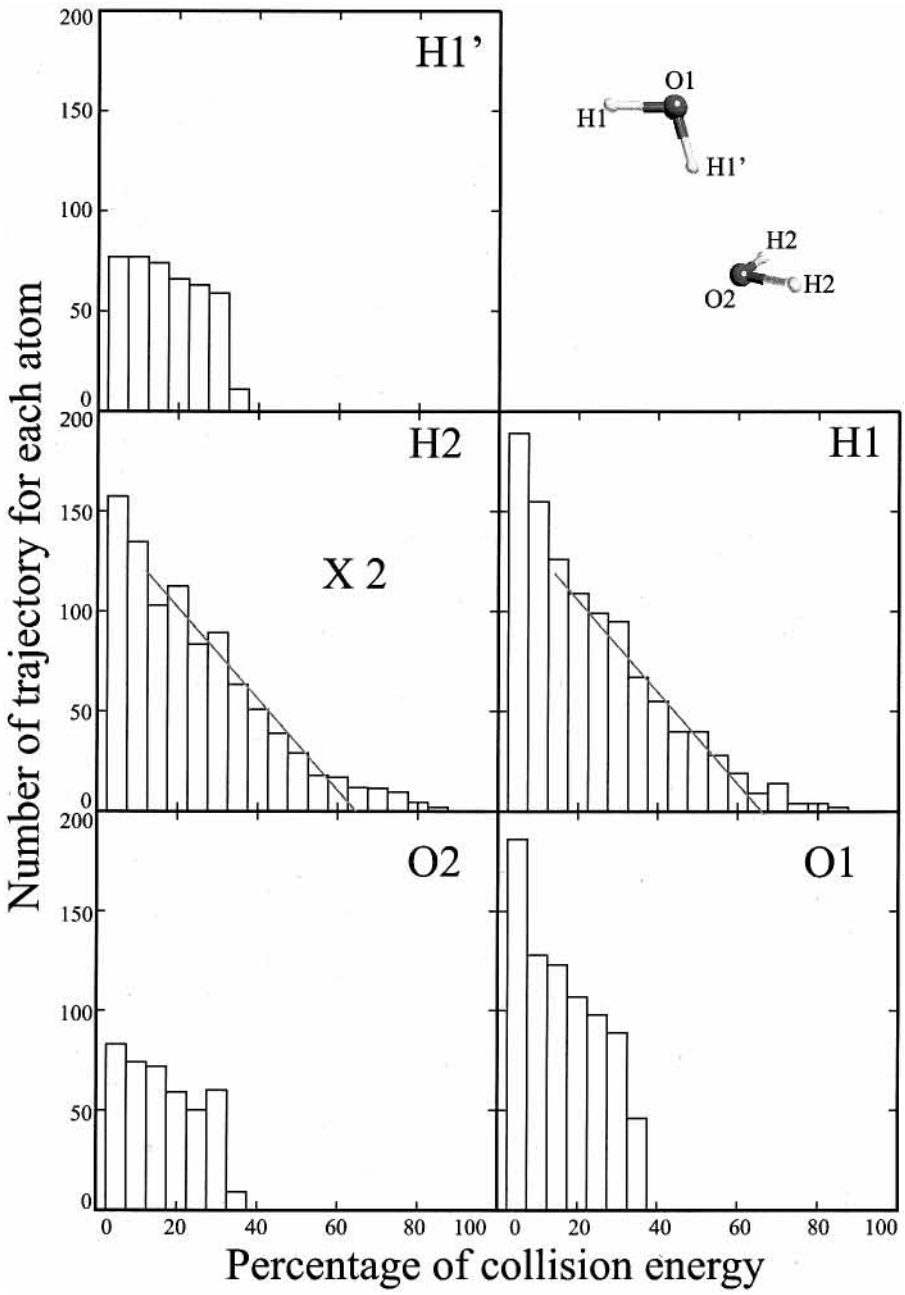

Figure 3. Histograms giving the number of trajectories that lead to a given percentage of the collision energy transferred into the water dimer by collisions with helium. Each histogram is labeled by the name of the cluster atom which is collided by helium. The cluster structure and the atom labeling are shown in the cartoon at the top right corner of the figure. The line in the histograms labeled H1 and H2 is to help the discussion.

The histograms describing the energy transfer to the various atoms of $(H_2O)_2$ are shown in Figure 3. Similarly, the histograms corresponding to the energy transfer into the isomers (a), (b), and (c) of $Na(H_2O)_3^+$ appear in Figures 4, 5, and 6, respectively. The structure of the cluster that is collided is recalled in each figure. Each atom of the cluster is labeled in the cluster scheme, as in the corresponding histogram. The symmetry of clusters (see Table 1) implies the equivalence of some atoms in each structure. For example, the six H-atoms of the most stable isomer or $Na(H_2O)_3^+$ are almost equivalent. The histograms of equivalent atoms are averaged in Figures 3−6. For clarity of the figures, the horizontal scale of the histograms is shown with a 5% sampling, whereas calculations have been performed with a higher resolution of 0.25%.

The vertical axis of each histogram gives the number of trajectories that leads to the percentage of energy transferred which is given in the horizontal axis of the Figure. A rapid examination of the histograms shows that their shape fall into three categories that are examined now. The first one corresponds to He colliding with a heavy atom (oxygen or sodium) and the two other when He collides with an H-atom.

Collision with Heavy Atoms. The left-hand side of the histograms shown in Figures 3−6, corresponds into a very small percentage of the energy transferred to the cluster and does not contribute that much to the CID cross section calculated in section 5. Hence, this part of the histograms does not need to be discussed extensively. Nevertheless, it contains a steric information on the accessibility of the various atoms of the clusters for large impact parameter trajectories. For example, in Figure 3, the accessibility of the oxygen atom O1 is larger than that of O2, which carries the H-bond. In Figure 4, the accessibility to the three equivalent O-atoms of isomer (a) is very small because of the steric hindrance due to sodium on one side and the H-atoms on the other. The O-atom labeled O2

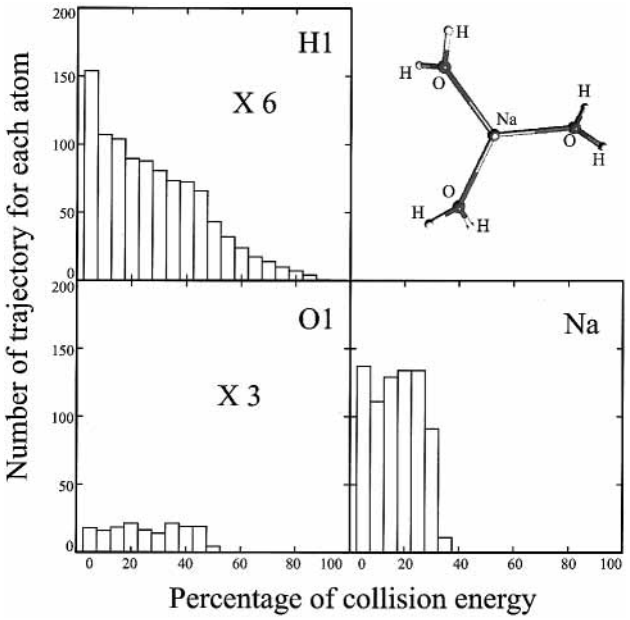

Figure 4. Same caption as Figure 3 for the $Na(H_2O)_3^+$ structure of lowest energy (isomer (a)).

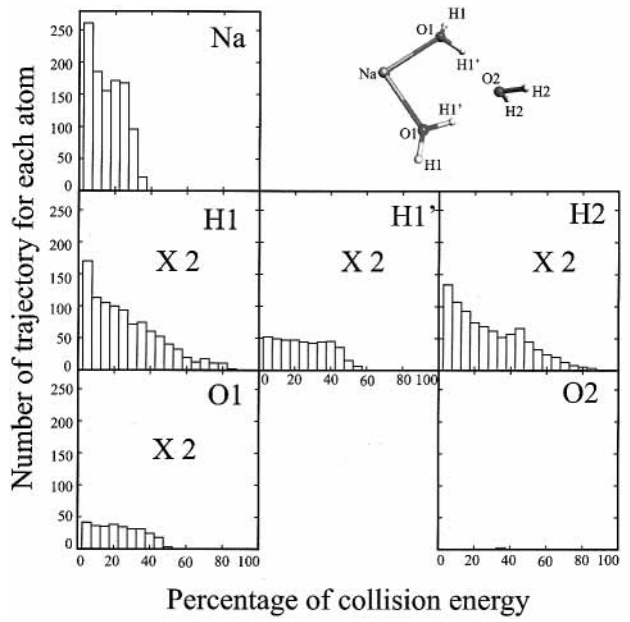

Figure 5. Same caption as Figure 3 for the isomer (b) of $Na(H_2O)_3^+$.

in Figure 5, which is involved in two "H-bonds", is almost not accessible. In Figure 6, the three O-atoms O1, O2, and O3 have almost the same histograms of those of the oxygen O1 atoms of Figures 5 and 4. Finally, the Na-atom, which is bonded to 2 water molecules, has about the same histogram as that of Na in Figure 5.

The relevant trajectories for the CID cross section calculated in section 5, end up with a significant percentage of energy transfer, say more than 20%.

The first important observation that can be done in Figures 3−6, is the sudden drop of the percentage of energy transfer at about 35−50% for the all the heavy atoms, O and Na. This upper limit of the energy transfer fits well with the impulsive model recalled in Appendix A.1. The model predictions are listed in Table 5. It appears that 40% (respectively 53%) of the collision energy goes into the O-atoms in collision with $(H_2O)_2$ (respectively $Na(H_2O)_3^+$) in agreement with the 38% (respectively 52%) observed in Figure 3 (respectively Figures 4−6) from the molecular dynamics calculations. Finally, the maximum energy transfer to sodium is only of 38% because of its larger mass than oxygen as describe by the impulsive model in Table 5 of Appendix A.1.

Interestingly also, the shape of the histograms associated with the heavy atoms, O and Na has a resemblance with that predicted by the line-of-center model, which is recalled in Appendix A.2. The fact that the calculated histograms differ from the ideal step functions predicted by the model can be attributed to the oversimplified hard sphere assumption of the line-of-center model.

Collision with H-Atoms. As mentioned above, the accessibility of the H-atom is given by the number of trajectories leading to a low percentage of energy transfer. We can check that the H-atom H1′, which is involved in the H-bond of $(H_2O)_2$ (figure 3) is less accessible than the three other H-atoms. A similar observation can be done with the H-atoms involved in the "H-bonds" of the isomers (b**)** and (c) of the $Na(H_2O)_3^+$ clusters (Figures 5 and 6).

The shape of the H-atom histograms differ substantially from that of the heavy atoms discussed above. Two types of histograms are observed whether they are associated with (i) a H-atom that is bonded only to an oxygen atom in a water molecule (H_i with $i = 1$, 2, or 3 in Figures 3−6). These H-atoms are named "Free H-atoms" hereafter; and (ii) a H-atom that is involved additionally in a H-bond or a "H-bond" (H_i' with $i =$ 1, 2, or 3 of Figures 3, 5, and 6). They are named "Bonded H-atom" in the following.

"Free H-Atom". The H-atoms labeled H1 and H2 in $(H_2O)_2$ do not play the same role in the structure in the cluster ion. This is apparent in the structure recalled in Figure 3. Nevertheless, they have a character in common: none of them is involved in an H-bond. Strikingly, the histograms associated with these H-atoms look very similar. Their shape can be resolved into two components: a quasi linear decay between 10 and about 60% is followed by a slower decay up to 90% energy transfer. A similar observation can be done when considering the H-atoms labeled H2 and H3 in Figures 4−6. Again none of these atoms are involved in a "H-bond".

The origin of the slow decay in the histograms is quite puzzling since it goes up to energy transfers larger than those predicted by the impulse model of Appendix A.1. An energy transfer of 64−69% of is predicted by the model, whereas up to 90% is observed in the histograms. The visualization of individual trajectories helps to unravel the origin of the slow decay. For this purpose, Figure 7 displays the percentage of energy transfer to the most stable structure of $Na(H_2O)_3^+$ as a function of the impact parameter of helium. The left-hand side of the Figure shows one of the face of the dodecahedral where the helium trajectories are initiated. The gray scale represents the percentage of energy transfer. The darkest zone corresponds to the largest energy transfer. The Figure shows that the transfer is maximum for the top-right water molecules and minimum for the bottom-right one. The bottom-right one is almost parallel to plane of the Figure, whereas the top-right is almost perpendicular to it. [The disposition of the water molecules with respect to the dodecahedral face appears in the 3D picture in right hand side of the figure.] From this, it appears that energy transfer is optimum when the initial velocity of helium is close to the direction of an O−H bond, with helium colliding the free H-atom at a non zero impact parameter. Such a collision transfers the collision energy as a rotation of the corresponding water molecule. A possible reason the energy transfer is so large

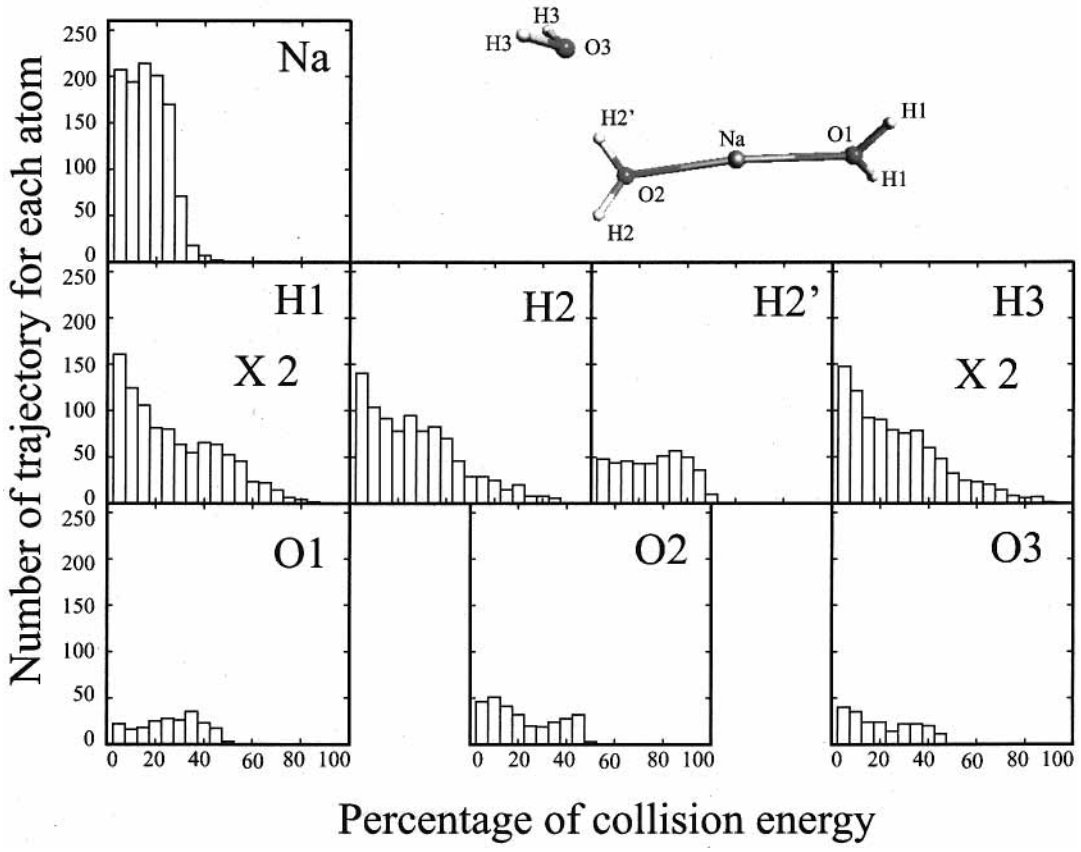

Figure 6. Same caption as Figure 3 for the isomer (c) of $Na(H_2O)_3^+$.

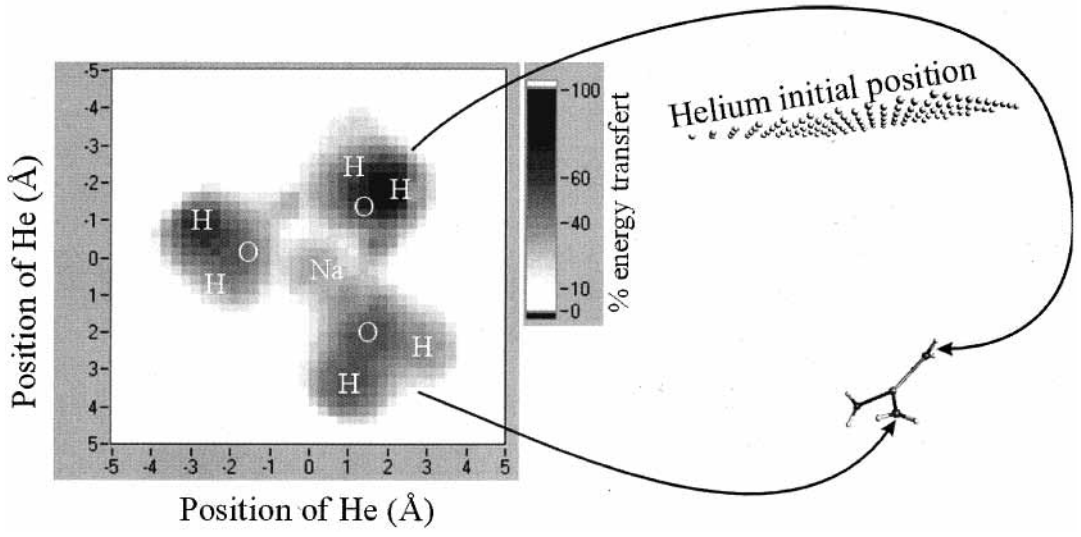

Figure 7. Impact parameter effect in the energy transfer between helium and the most stable structure of $Na(H_2O)_3^+$ (isomer (a)). The figure on the left represents one of the dodecahedral faces where the trajectories are initiated. The 3D representation of this initial conditions can be seen on the right-hand side of the Figure which has been tilted by about 90° with respect to the left-hand side of the Figure. The gray scale in the left figure is darker when the percentage of energy transfer is larger. The cluster structure that appears in white in the figure is a projection on the dodecahedral face. The bottom right water molecule is almost parallel to the dodecahedral face (plane of the figure) as seen in the figure on the right, whereas the top right one is close to perpendicular to this surface. The initial velocity of helium is perpendicular to the plane of the figure.

in this case, is the He−H collision which cannot be represented as purely impulsive. The water molecule is indeed likely to start rotating during the collision with helium. This corresponds to helium feeling a less repulsive apparent potential. Hence, the recoil velocity of helium is smaller, and the energy transfer to the water molecule is enhanced. Of course, such a classical picture of the water rotation should be regarded with caution, owing to the inherent quantal character of rotations in such a light system. Anyway, the number of impact parameters that lead to such a transfer is quite small and explains why only a small number of trajectories corresponds to energy transfers larger than 60%.

"Bonded H-Atom". The other type of H-atoms are involved in a H-bond (H′1 in Figure 3) or in a "H-bond" (H′1 and H′2 in Figures 5 and 6). The histograms corresponding to these atoms do not exhibit the tail at large energy transfer. This is easy to rationalize, taking the origin of the tail discussed above.

These atoms indeed cannot be accessed along an H−O bond because of the steric hindrance.

In fact, the shape of these histograms is close to that encountered above for the heavy atoms. There is a difference however. The impulsive model predict a maximum energy transfer that is larger than observed in the MD calculations, more than 60% versus about 50%. A possible reason for that is the steric effect due to the "H-bonded" water molecules. The only access to the "H-bonded" H-atom is indeed to arrive almost perpendicularly to the plane of the water molecule to which it belongs. This does not allow for a pure head on collision with respect to the H-atom because the van der Waals radius of oxygen is larger than the length of the OH bond in the water molecule. As a result, He atom can hit the H-atom only when having a non zero impact parameter with respect to the H-center. A reduced energy transfer is expected in this case.

5. Prediction of Cross Sections for Collision-Induced Dissociations

When the energy transferred collisionally into the cluster exceeds the binding energy of a water molecule, a dissociation should occur. If the excess energy is small and if the cluster has a large number of degrees of freedom this could take time and be even not observable experimentally if the time window of the experiment is not sufficient.[5,6] The question of a time window for dissociation also appears in the present calculations. Trajectories are followed indeed for only 900 fs in the He + $Na(H_2O)_3^+$ collisions. Within this time window, although dissociation is certain, only few trajectories end up with the loss of a water molecule. This question is examined further in section 6. The point here is to calculate the energy dependence of CID cross sections, given the histograms presented and discussed in the previous sections. This is done first for the $(H_2O)_2$ and $Na(H_2O)_3^+$ + He collisions where histograms have been calculated. The calculation is then extended to the more general $M(H_2O)_n^+$+He collision and applied to $Au(H_2O)_{1,2}^+$ + He.

5.1. Cross Sections for $(H_2O)_2$ and $Na(H_2O)_3^+$ + He CID. The histograms describing the energy transfer have been sorted in the previous section for the individual atoms of the $(H_2O)_2$ and $Na(H_2O)_3^+$ clusters. Of course a global histogram describing the energy transfer toward the entire cluster is also given by the calculation. The global histogram associated to the filament isomer (isomer (c)) of $Na(H_2O)_3^+$ is shown in Figure 8.

The following set of assumptions enables the global histograms to predict the energy dependence of CID cross sections.

1. When energy is transferred into the cluster, above the threshold energy to lose a water molecule, the cluster actually dissociates.

2. The bottom scale of the global histogram, when multiplied by the collision energy, becomes the absolute amount of energy transferred into the cluster. It is shown as the top axis in Figure 8. This is justified by the impulse character of the energy deposition into the cluster.

3. Then, all the trajectories which transfer more energy into the cluster than needed for removing a water molecule are counted into the CID cross section. This corresponds to the sum of all the trajectories that are to the right of the vertical line labeled "Energy threshold" in Figure 8.

4. As a final step, the absolute value of the CID cross section is obtained by multiplying this number by the elementary cross section (5.2×10^{-3} Å^2) which corresponds to the present sampling of the trajectories.

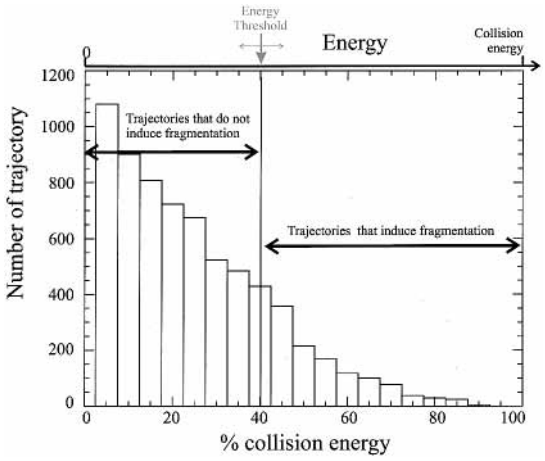

Figure 8. Histogram giving the total energy transfer to the filament isomer (isomer (c)) of $Na(H_2O)_3^+$. It is the proper sum of the histograms that appear in Figure 6. The bottom scale gives the percentage of the collision energy that is transferred collisionally into the cluster, the top scale gives the absolute amount of energy transferred, the highest value being the collision energy. The vertical line corresponds to the threshold energy for loosing a water molecule. It moves to the left-hand-side of the figure when higher and higher collision energies are considered.

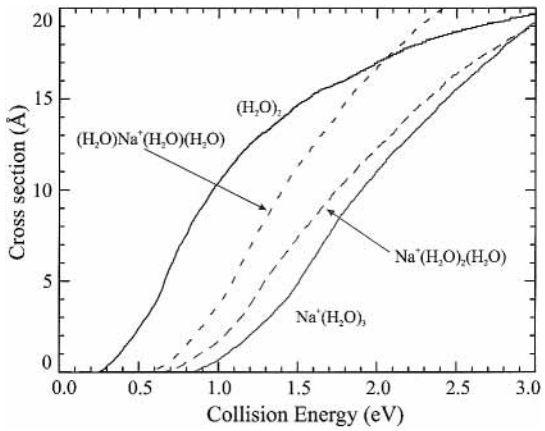

Figure 9. CID cross sections as a function of the collision energy. The four curves refer to collision of helium with $(H_2O)_2$ and the isomers (a) $(Na^+(H_2O)_3)$, (b) $(Na^+(H_2O)_2(H_2O))$, and (c) $((H_2O)Na^+(H_2O)(H_2O))$ of $Na(H_2O)_3^+$ as labeled in the figure.

The energy dependence of the CID cross sections as calculated for collisions of helium with $(H_2O)_2$ and the isomers (a), (b) ,and (c) of $Na(H_2O)_3^+$ are shown in Figure 9. At threshold, the contributions originate essentially from collisions where the energy is transferred toward H-atoms that are not involved in an "H-bond". The percentage of energy transfer is indeed maximum for these atoms.

To our knowledge, no detailed energy dependencies of CID cross sections in He + $Na(H_2O)_3^+$ collisions exists from experiments that can be compared to the present calculation. The experimental and theoretical information that is available in the literature for energy transfers in helium + water cluster collisions corresponds to too small collision energies (in the 0.005−0.02 eV range) to allow relevant comparisons with the present work.[43,44]

5.2. Generalization to $M(H_2O)_n^+$ + He CID: An Application to $Au(H_2O)_{1,2}^+$ + He Collisions. The more general $M(H_2O)_n^+$ + He collisions are considered here. No global histogram describing the energy transfer to these clusters has been calculated. Nevertheless, from the discussion of the He + $Na(H_2O)_3^+$ collisions, the nature of the metal ion core does not

seem to play an important role, except for the mass difference. Moreover, the energy transfer appears as local and sensitive to the local environment of the atoms ("H-bonded" or not) that are collided. Hence, it seems possible to use the histograms calculated for the $Na(H_2O)_3^+$ + He collisions in the more general context of $M(H_2O)_{1,2}^+$+He collisions. Certainly, these histogram have to be corrected to account for the mass difference between M and Na. This is done hereafter, taking the $Au(H_2O)_{1,2}^+$ cluster ions as an example. Detailed experimental data are available indeed for these collisions.[20] As we shall see, doing so offers a procedure to extract meaningful information on the Au and $Au(H_2O)_2^+$ binding energies from the CID experimental data, the reliability of which can be tested using the ab initio results reported in section 3.

The first step toward this goal is to assume a structure to the cluster. For instance, two different structures can be imagined for $Au(H_2O)_2^+$: the most stable, having the two water molecules in the first shell and the another one having one water molecule in the first shell and the other in the second shell. For example, the second structure has one heavy ion (Au^+), two O-atoms, one H-atom involved in an "H-bond" and three H-atoms that are not involved in an "H-bond".

The second step is coming from the fact that changing the ion mass from Na^+ to Au^+ certainly changes the histograms of energy transfer from those calculated for He + $Na(H_2O)_3^+$ collisions, simply because the maximum energy transfer scales as suggested by the impulse model (see Appendix A.1 and Table 3). A first way (hereafter called the *recalculating* procedure) to account for this is to rerun the molecular dynamics calculation, just replacing the mass of sodium by that of Au. The histograms that are obtained, thus serve has "universal" histograms to describe the energy transfer to the Au-, O-, and H-atoms, according to their local environment, i.e., involved in an "H-bond" or not. A second way to account for the replacement of Na^+ by Au^+ needs almost no calculations. It is called hereafter the *scaling* procedure) The idea is to use histograms describing the He + $Na(H_2O)_3^+$ collisions, and just scale the percentage of energy transfer, according to the impulsive model recalled in Appendix A.1 to account for the heavier mass of the gold ion. Helium makes indeed an elastic collision with the metal ion core and the energy scale of the corresponding histogram can be adapted according to the reduced mass of the He−metal ion pair. The maximum energy transfer that is expected in this case is shown in Table 5. It is very small for the gold ion. It is only marginally affected for the other atoms when switching from Na^+ to Au^+.

The third step is to sum these histograms, whatever the way they have been obtained, according to the structure that has been assumed for the cluster. For example, with the filament structure of the $Au(H_2O)_2^+$ ion, $Au^+(H_2O)(H_2O)$, one has to sum one histogram corresponding to the heavy ion (Au^+), twice the histogram for an O-atom, one histgram for an H-atom involved in a "H-bond" and three times the histogram for a H-atom that is not involved in a "H-bond". This provides us with the global histogram describing the energy transfer toward the filament isomer of $Au(H_2O)_2^+$.

The final step is to calculate the energy dependence of the CID cross section, as explained in the previous section. The difference here is that the incremental binding energy of water is not known here. Instead, it is used here as a parameter to fit the experimental results in order to get the energetics information on the ion from the experimental results.[4]

[In order to get a reliable fit, the comparison between the calculated CID cross section and the experimental one must account for the experimental dispersion of the collision energy. The dispersion due to the dispersion of the ion kinetic energy in the ion beam is negligible under the experimental conditions of ref 20. In contrast, the effect of the thermal motion of helium at $T = 300$ K is not negligible. It is accounted for by averaging the calculated CID cross section sigma according to

$$\hat{\sigma}(E_{coll}) = \int_0^{\pi} \sigma \left(E_{coll} + {}^3/_2 k_B T \frac{m_{He}}{m_{He} + m_C} + \sqrt{{}^3/_2 k_B T \frac{m_{He}}{m_{He} + m_C} + E_{coll} \cos\theta} \right) (\sin\theta)/2 \, d\theta \quad (1)$$

where m_{He} is the mass of helium, m_C that of the cluster ion, and E_{coll} is the collision energy when assuming a fixed helium target.]

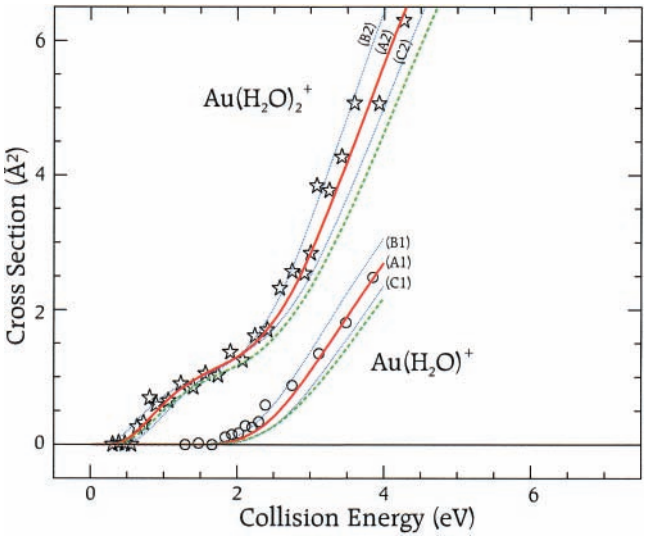

Figure 10. Energy dependence of the CID cross-section in He + Au and He + $Au(H_2O)_2^+$ collisions. The experimental results of ref 20 are given by the open circles and stars, respectively. The corresponding best fits by the procedure explained in the text are shown as the solid curves labeled A1 and A2. A1 is associated with 1.74 eV binding energy for the water molecule in Au. A2 assumes the presence of a filament isomer and a compact one in the ratio 1:9 with incremental binding energies of 0.4 and 1.95 eV, respectively. The dotted curves labeled B1 and C1 on one hand, B2 and C2 on the other are used to estimate the errors bars on the binding energies. The dashed curve shows the CID cross section predicted by the scaling procedure (see text) when using the fit parameters above.

The energy dependence of CID cross sections measured experimentally, both for Au and $Au(H_2O)_2^+$ in ref 20 are shown in Figure 10. They are compared to best fits, shown as solid lines A1 and A2 in the figure when the histograms are obtained by the *recalculating* procedure. The sensitivity of the fit in determining binding energy is illustrated by the dotted curves obtained when changing the binding energies by 0.1 eV for the first threshold and 0.15 eV for ther second (compare the curve A1 to the curves B1,C1 on one hand and A2 to (B2,C2) on the other).

The energy dependence of the CID cross section that is calculated when using the *scaling* procedure to get the histograms is shown in Figure 10 as the dashed curves. It uses the best fit parameters obtained using the *recalculating* procedure. A significant disagreement is observed which would result into a 25% underestimation of the binding energies if the scaled histograms were used to fit the experimental results. The origin

TABLE 4: Energetics (eV) for the $Au(H_2O)_{1,2}^+$ Systems

	D_e			ΔD_e		D_0	ΔD_0
cluster	this work	ref 42	ref 41	this work	ref 42	this work	this work
$Au(H_2O)^+$ C_s	1.56	1.74[a]	1.68[b] (1.56)[b]			1.47	
$(H_2O)Au(H_2O)^+$ C_2	3.54			1.98	2.09[a]	3.29	1.82
$Au(H_2O)(H_2O)^+$ C_s	2.24			0.68		2.03	0.56

[a] Estimated complete basis set (CBS) CCSD(T) limit. This value is obtained from the CBS MP2 limit given by extrapolating the average between the cp-uncorrected and the cp-corrected binding energies and correcting for higher-order correlation recovery. [b] MP2 level and in parentheses partially reoptimized CCSD(T) level. Theses values are calculated without taking into account the BSSE.

of this is due to the ambiguity already mentioned when assigning the energy transfer to the cluster atom which had the closest approach distance with helium during the collision, in cases where helium makes several collisions within the cluster. The effect that is observed here is due to trajectories where helium makes a first collision with Na^+, transferring almost no energy and a second one with an O-atoms where energy is transferred. In such a case, the energy transfer is assigned incorrectly to Na and is scaled to zero when switching from Na^+ to Au^+ because of the mass ratio. This results into a poorer energy transfer than normal, and explains the underestimation of the CID cross section observed in Figure 10 when comparing the dashed curve to the solid one. This effect is dramatic here because of the large mass difference between Na and Au. Instead, when switching from Na to a metal, the mass of which is only a factor 2 or 3 different (a transition metal of the first raw for instance), the effect can safely be ignored and the *scaling* procedure is accurate enough to get reliable CID cross sections. As a policy, we can consider that the histograms calculated for gold are adequate for describing the energy transfer toward cluster carrying an heavy metal ion, of course after scaling if the ion is not gold. Similarly the histograms calculated for sodium are adequate when the metal ion is a light one. In the present context, only the results obtained using the *recalculating* procedure are discussed further.

The agreement between the best fit curve A1 and the experimental results for Au is excellent. The corresponding best fit value of the Au^+-H_2O binding energy, 1.74 ± 0.1 eV, is fully consistent with the theoretical values reported in Table 4. This appears as a first validation of the procedure used here to extract binding energies from the CID experiment.

When turning to the $Au(H_2O)_2^+$ cluster, it must be recalled that two isomers have been found in our experimental work,[20] one corresponding to first shell water molecules with no "H-bond" present ($(H_2O)Au^+(H_2O)$) and the other to a filament structure involving an "H-bond" ($Au^+(H_2O)(H_2O)$). As said above, the two isomers lead to a different summation of the histograms because the local environment of the H- and O-atoms is not the same in both isomers. Hence, the energy dependence of the CID cross section is different for both. The best fit curve A2 involves three fit parameters: (i) the population ratio between both isomers, (ii) the incremental binding energy of water in the ($(H_2O)Au^+(H_2O)$) isomers, and (ii) that in the filament isomer $Au^+(H_2O)(H_2O)$. The best fit leads to the following results: the filament isomer corresponds to $10 \pm 2\%$ of the cluster ion beam; the incremental binding energies are 0.4 ± 0.1 eV for the filament isomer $Au^+(H_2O)(H_2O)$ and up to 1.95 ± 0.15 eV for the most stable isomer $(H_2O)Au^+(H_2O)$. These incremental binding energies are in fair agreement with those obtained from the ab initio calculations reported in the last column of Table 4. This validates further the procedure used to extract incremental binding energies from measured energy dependence of CID cross section in $He + M(H_2O)_n^+$ collisions.

Before leaving this section, it is important to outline that the fit to the experimental data is not restricted to the threshold region of the CID cross section. Instead, since the energy dependence of the cross section is well accounted by the present model, the parameters of the fit (binding energies and relative abundance of the isomer) are adjusted so as the energy dependence of the cross section is well reproduced above threshold. This certainly reduces uncertainties on the fitted binding energies that are due to the effects that normally affect the reliability of the measured CID cross sections near threshold: the weakness of the cross section and internal energy of the cluster in particular.

6. Toward a Fragmentation Model

We turn back here to the $Na(H_2O)_3^+$ and $(H_2O)_2$ clusters. As mentioned above, within the calculation time, most of the trajectories do not show dissociation even when it is energetically possible. For most trajectories indeed, the dissociation mechanism is evaporation and the evaporation time exceeds the time during which the trajectories were followed. This is especially true for the $Na(H_2O)_3^+$ clusters, since they have substantially more degrees of freedom than the water dimers. For the latter indeed the distinction, based on collision time between evaporation and impulsive dissociation is not clear. Remembering that the energy transfer to the cluster is essentially impulsive, it thus appears that the dominant dissociation process is the two step impulsive mechanisms (IM2) recalled in the Introduction.[17] This results fit well with the commonly accepted picture where CID is a two-step process[2,45]

$$\begin{aligned} A^+(\nu\,0) + P &\xrightarrow[\text{impulse}]{} A^+(\nu^*) + P \\ &\downarrow \text{(slow)} \\ &A_1^+ + A_2 \end{aligned} \qquad (2)$$

where A^+ is the parent cluster, A_1^+ and A_2 its fragments, and P the projectile.

Nevertheless, besides this dominant process, trajectories exist in the calculation, which correspond to a direct dissociation. The associated mechanism is therefore the direct impulsive mechanism (IM1) when following the classification of dissociation mechanisms proposed in the group of Barat and Fayeton.[17] Hence, the calculated trajectories were also sorted for determining the impulsive dissociation cross section in $He + Na(H_2O)_3^+$ collisions. The criterion to decide of an impulse dissociation is that one of the water molecule is at more than 7 Å from the ion core at the end of the calculation (900 fs). For the filament species, the isomer (c), a cross section of 0.7 $Å^2$ was found at a collision energy of 1.26 eV. This corresponds to 11% of the total fragmentation cross section. In this case, the collision give an impulse to the collided atom in the direction of a dissociation coordinate, with the consequence that most of the collision energy goes as translation of the water molecule that has been collided. Indeed, translation seems much better coupled to the dissociation coordinate than rotation. This has three consequences: (i) rather few impact parameters lead to such energy transfer; (ii) when the collision energy is in excess with respect to the dissociation energy, only a small part of the collision energy is kept by the cluster for a further loss of water. Instead, the excess collision energy is given to the departing water

molecule as kinetic energy; (iii) the water binding energy that has to be taken in to consideration is the activation energy of the direct dissociative coordinate rather than the adiabatic one. This energy can be estimated by the difference between the total energy of the initial $M(H_2O)_n^+$ cluster and the total energy of $M(H_2O)_n^+ - 1$ cluster keeping the same geometry as $M(H_2O)_n^+$ except for the less bonded water molecule that has been removed. In system where the direct IM1 mechanism has an overriding importance, the measured threshold energy for dissociation could be biased and fall between this limit and the adiabatic binding energy.

An interesting phenomenon occurs for trajectories having an impact parameter not exactly matching the condition for a direct dissociation mechanisms (IM1). In this case, part of the collision energy serves to heat the cluster. The collided water molecule still starts to leave the cluster but without enough energy to actually leave the attraction of the ion core. The water molecule thus turns back, collides with the hot cluster moiety, and all the energy transferred to the cluster is then randomized before the dissociation. This is the two-step direct impulsive mechanism (IM2). Of course, when the collision energy is increased the same impact parameter leads to the IM1 dissociation mechanism. There is therefore a continuous shift from IM2 to IM1 as the collision energy is increased.

7. Conclusion

Molecular dynamics calculations were performed to simulate the collisions between an helium atom and an $(H_2O)_2$ or a $Na(H_2O)_3^+$ cluster. Three different geometries of the $Na(H_2O)_3^+$ clusters were considered. That of lowest energy has the three water molecules in the first solvation shell. They are directly bonded to the metal ion. The two other geometries have one water molecule in the second solvation shell. One of these isomers has the filament structure $(H_2O)Na^+(H_2O)(H_2O)$.

The work has documented the partial conversion of the collision energy into internal excitation of the cluster. The water molecules were treated as a rigid five-center systems. The interaction energy between the cluster subunits, water and metal ion, were calculated via a model potential which includes all the important contributions: electrostatic, polarization, repulsion, and dispersion. Comparatively, the molecular dynamics program is fairly standard.

The calculations consisted in sampling trajectories to determine how the collision energy, which is transferred as an impulse to the cluster, is actually deposited on one of the atoms of the cluster. More precisely, an histogram is constructed for each atom of the cluster which gives the number of trajectories responsible for a given transfer of energy to this atom. Of course the energy transfer to heavy species, O and Na, is limited whereas up to 90% of the collision energy can be transferred to an H-atom. The important point is elsewhere. It appears that the energy transfer to a H-atom, depends crucially of its local environment, whether it is involved or not in an "H-bond". The amount of energy transferred goes up to 90% toward a a non "H-bonded" H-atoms, whereas it is less than 60% toward an "H-bonded" H-atom.

The above histograms allowed us to predict the energy dependence of the CID cross section in $Na(H_2O)_3^+ + He$ collisions. More importantly, they can be proposed as bricks allowing to construct a global histogram which describes the energy transfer in the more general $M(H_2O)_n^+ + He$ collisions (M is a metal atom) and to calculate the energy dependence of the corresponding CID cross section. An application was done for $He + Au$ and $He + Au(H_2O)_2^+$ collisions offering a procedure to extract meaningful information on the binding energy of the most weakly bonded water molecule in these clusters.

The important point that must be outlined here is that the fit to the experimental data using the molecular dynamics calculation provides information that can be directly compared to theoretical calculations: structures and incremental binding energies of the $M(H_2O)_n^+$ cluster ions. The only fit parameter that cannot be simply compared to calculation is the abundance ratio between various isomers when present in the beam. Importantly also, the fit to the experimental data that is allowed by the present model is not restricted to the threshold energy region of the CID cross section. Instead, the parameters of the fit are adjusted so as the model well reproduces the experimental data way above threshold, in a region where the experiment signal are often more reliable.

TABLE 5: Maximum Percentage of Energy Transferred to the Various Atoms of the $(H_2O)_2$, $Na(H_2O)_3^+$, and $Au(H_2O)_2^+$ Clusters in Collisions with Helium[a]

	H	O	Na or Au
$(H_2O)_2$	69%	40%	
$Na(H_2O)_3^+$	66%	53%	37%
$Au(H_2O)_2^+$	64%	60%	1.2%

[a] The values are calculated using expression 3. The results for gold are used in section 5.2.

Acknowledgment. The authors acknowledge the C.E.A. that has supported this work under the grant "Interaction ion métallique molécule".

Appendix A. Energy Transfer Models

A.1. Impulse Model. Several impulse models are available in the literature to describe collisions which transfer energy from the translation into molecular vibration, T-to-V energy transfers. Let us cite that of Mahan[10] on atom−diatom collisions, and a molecular model due to Uggerud and Derrick,[11] which reduces a polyatomic target to a pseudo-diatom. The later model predicts that the maximum of the T-to-V energy transfer occurs for an head on collision of the atomic projectile A on an atom labeled B_i of the polyatomic target B. The corresponding percentage of T-to-V energy transfer is given by

$$\%E_{max} = 4 \frac{m_{Bi} m_A}{(m_{B_i} + m_A)^2} \frac{m_B - m_{B_i}}{m_B} \frac{m_B + m_A}{m_B} \qquad (3)$$

where m_A is the mass of the projectile, m_B the mass of the polyatomic target, and m_{Bi} the mass of the atomic subunit of the target that is collided by the projectile.

Expression 3 can be applied to the present He-cluster collisions. It predicts a different value for $\%E_{max}$, whether a H, an O, or the metal ion core is collided by He. The model predictions are displayed in Table 5.

A.2. Line-of-Centers Model. The line-of-center model is another venerable tool in reaction dynamics.[46,47] It is probably the simplest model that has been designed to account for the energy dependence of reactive cross-sections (a simple dissociation in the present case) when a step barrier has to be surmounted (here, the endoergicity barrier of the dissociation). It is a hard sphere model of the collision between an atom A and molecule B, which considers that all the kinetic energy corresponding to the movement along the line-of-center connecting the center of A to that of B can be trapped by B to turn on the reaction. In the present context of He (i.e., A)−cluster

(i.e., B) collisions, the line-of-center energy is transferred into B as internal excitation. This is the first step of the model. The second step would be dissociation of the cluster. Let stay at the first step for the moment. With this in mind, the fraction E_t/E of the collision energy E that is transferred into B is given by

$$\frac{E_t}{E} = 1 - \frac{b^2}{R^2} \tag{4}$$

where b is the impact parameter of helium on the cluster and R a reasonable hard sphere radius for the He-cluster collision. Expression 4 must now be related to an histogram in order to compare its predictions to the calculations of the present work. Let ρ_0 be the number of trajectories per unit surface ($\rho_0 = 1/(5.2 \times 10^{-3})$ in the framework of the calculations performed for $Na(H_2O)_3^+$). The histogram representation of the calculation then corresponds to sample the energy by increments ΔE and to determine the number of trajectories $\Delta(\rho_0 \pi b^2)$ which lead to an energy transfer ranging between $E_t - \Delta E/2$ and $E_t + \Delta E/2$. The histogram $H(E_t)$ is therefore given by

$$H(E_t) = |\int_{E_t - \Delta E/2}^{E_t + \Delta E/2} \rho_0 \pi \mathrm{d}b^2(E_t)| \tag{5}$$

$$= \rho_0 \pi |\int_{E_t - \Delta E/2}^{E_t + \Delta E/2} - \mathrm{d}\left(R^2 \frac{E_t}{E}\right)| \tag{6}$$

$$= \rho_0 \frac{\pi R^2}{E} \int_{E_t - \Delta E/2}^{E_t + \Delta E/2} \mathrm{d}\, E_t \tag{7}$$

$$= \rho_0 \pi R^2 \frac{\Delta E}{E} \tag{8}$$

$H(E_t)$ does not vary with the amount of energy $E_t$transferred to the cluster, $\rho_0 \pi R^2$ being the number of trajectories where helium collides the target cluster. If choosing ΔE as a percentage of the collision energy E, the histogram $H(\%E_t)$ values are almost equivalent to those calculated in the molecular dynamics simulation. The only thing to add is the constrain due to the mass ratio between helium and the atom of the cluster that is collided. It is given by the impulse model of Appendix A.1. In doing so, the line-of-center model predicts histograms for the energy transfer as a step function: the number of trajectories leading to a given percentage of energy transfer is constant, up to a maximum percentage.

References and Notes

(1) Cooks, R. G. *Collision Spectroscopy*; Plenum Press: New York, 1978.

(2) Shukla, A. K.; Futrell, J. H. *J. Mass Spectrom.* **2000**, *35*, 1069.

(3) Rodgers, M. T.; Armentrout, P. B. *Mass Spectrom. Rev.* **2000**, *19*, 215.

(4) Dalleska, N. F.; Honma, K.; Armentrout, P. B. *J. Am. Chem. Soc.* **1993**, *115*, 12125.

(5) Rodgers, M. T.; Ervin, K. M.; Armentrout, P. B. *J. Chem. Phys.* **1996**, *106*, 4499 1996.

(6) Rodgers, M. T.; Armentrout, P. B. *J. Chem. Phys.* **1998**, *109*, 1878.

(7) Aristov, N.; Armentrout, P. B. *J. Phys. Chem.* **1986**, *90*, 5135.

(8) Freasier, B. C.; Jolly, D. L.; Hamer, N. D.; Nordholm, S. *Chem. Phys.* **1986**, *106*, 413.

(9) Meroueh, O.; Hase, W. L. *J. Phys. Chem. A* **1999**, *103*, 3981.

(10) Mahan, B. H. *J. Chem. Phys.* **1970**, 52, 5221.

(11) Uggerud, E.; Derrick, P. J. *J. Phys. Chem.* **1991**, *95*, 1430.

(12) Shin, H. K. Vibrational Energy Transfer. In *Dynamics of Molecular Collisions, Part A*; Miller, W. H., Ed.; Modern Theoretical Chemistry, Plenum Press: New York, 1976.

(13) de Sainte Claire, P.; Peslherbe, G. H.; Hase, W. L. *J. Phys. Chem.* **1995**, *99*, 8147.

(14) de Sainte Claire, P.; Hase, W. L. *J. Phys. Chem.* **1996**, *100*, 8190.

(15) Barat, M.; Brenot, J. C.; Dunet, H.; Fayeton, J. A. *Z. Phys. D* **1997**, *40*, 323.

(16) Barat, M.; Brenot, J. C.; Dunet, H.; Fayeton, J. A.; Picard, Y. J.; Sizun, M. *Chem. Phys. Lett.* **1999**, *306*, 233.

(17) Barat, M.; Brenot, J. C.; Dunet, H.; Fayeton, J. A.; Picard, *J. Chem. Phys.* **1999**, *110*, 10758.

(18) Babikov, D.; Sizun, S.; Aguillon, F.; Sidis, V. *Chem. Phys. Lett.* **1999**, *306*, 226.

(19) Sublemontier, O.; Poisson, L.; Pradel, P.; Mestdagh, J.-M.; Visticot, J.-P. *J. Am. Soc. Mass Spectrom.* **2000**, *11*, 160.

(20) Poisson, L.; Pradel, P.; Lepetit, F.; Réau, F.; Mestdagh, J.-M.; Visticot, J.-P. *Eur. Phys. J. D.* **2001**, *14*, 89.

(21) de Pujo, P.; Mestdagh, J.-M.; Visticot, J.-P.; Cuvellier, J.; Meynadier, P.; Lallement, A.; Berlande, J. *Z. Phys. D.* **1993**, *25*, 357.

(22) Gaigeot, M.-P.; de Pujo, P.; Brenner, V.; Millié, Ph. *J. Chem. Phys.* **1997**, *106*, 9155.

(23) Gaigeot, M.-P. Thèse de l'Université Paul-Sabatier, Toulouse, France, 1997.

(24) Verlet, L. *Phys. Rev. A* **1967**, *25*, 978.

(25) Fincham, D. *Mol. Simul.* **1992**, *8*, 165.

(26) Claverie, P. in *Intermolecular Interactions from Diatomics to Biopolymers*; Pullman, B., Ed.; Wiley: New York, 1978.

(27) Hess, O.; Caffarel, M.; Langlet, J.; Caillet, J.; Huiszoon, C.; Claverie, P. in *Proceedings of the 44*th *International meeting Modelling of Molecular Structures and Properties in Physical Chemistry and Biophysics*, Nancy, France, Sept 11−15, 1989; Rivail, J.-L., Ed.; Elsevier: Amsterdam, 1990.

(28) Brenner, V. Thèse de l'Université de Paris-sud, Paris, 1993.

(29) Brenner, V.; Millié, Ph. *Z. Phys. D.* **1994**, *30*, 327.

(30) Derepas, A.-L.; Soudan, J.-M.; Brenner, V.; Millié, Ph. *J. Comput. Chem.* **2001**. In press.

(31) Vigne-Maeder, F.; Claverie, P. *J. Chem. Phys.* **1988**, *88*, 4934.

(32) van Duijneveldt, F. B. IBM Research Report RJ945; 1971.

(33) Xantheas, S. S. *J. Chem. Phys.* **1995**, *102*, 4505.

(34) Schütz, M.; Brdarski, S.; Widmark, P.-O.; Lindh, R.; Karlström, G. *J. Chem. Phys.* **1997**, *107*, 4597.

(35) Curtiss, L. A.; Frurip, D. J.; Blander, M. *J. Chem. Phys.* **1979**, *71*, 2703.

(36) Reimers, J. R.; Watts, R. O.; Klein, M. L. *Chem. Phys.* **1982**, *64*, 95.

(37) Bertolus, M.; Brenner, V.; Millié, Ph.; Maillet, J.-B. *Z. Phys. D* **1997**, *39*, 239.

(38) Dalleska, N. F.; Tjelta, B. L.; Armentrout, P. B. *J. Phys. Chem.* **1994**, *98*, 4191.

(39) Roos, R. B.; Powers, J. M.; Atashroo, T.; Ermler, W. C.; John, L. A.; Christiansen, P. A. *J. Chem. Phys.* **1990**, *93*, 6654.

(40) Frisch, M. J.; Trucks, G. W.; Schlegel, H. B.; Scuseria, G. E.; Robb, M. A.; Cheeseman, J. R.; Zakrzewski, V. G.; Montgomery, J. A.; Stratmann, R. E.; Burant, J. C.; Dapprich, S.; Millam, J. M.; Daniels, A. D.; Kudin, K. N.; Strain, M. C.; Farkas, O.; Tomasi, J.; Barone, V.; Cossi, M.; Cammi, R.; Mennucci, B.; Pomelli, C.; Adamo, C.; Clifford, S.; Ochterski, J.; Petersson, G. A.; Ayala, P. Y.; Cui, Q.; Morokuma, K.; Malick, D. K.; Rabuck, A. D.; Raghavachari, K.; Foresman, J. B.; Cioslowski, J.; Ortiz, J. V.; Stefanov, B. B.; Liu, G.; Liashenko, A.; Piskorz, P.; Komaromi, I.; Gomperts, R.; Martin, R. L.; Fox, D. J.; Keith, T.; Al-Laham, M. A.; Peng, C. Y.; Nanayakkara, A.; Gonzalez, C.; Challacombe, M.; Gill, P. M. W.; Johnson, B. G.; Chen, W.; Wong, M. W.; Andres, J. L.; Head-Gordon, M.; Replogle, E. S.; Pople, J. A. *Gaussian 98*; Gaussian, Inc.: Pittsburgh, PA, 1998.

(41) Hruák, J.; Schröder, D.; Schwarz, H. *Chem. Phys. Lett.* **1994**, *225*, 416.

(42) Feller, D.; Glendening, E. D.; de Jong, W. A. *J. Chem. Phys.* **1999**, *110*, 1475.

(43) Brudermann, J.; Buck, U.; Fredj, E.; Gerber, R. B.; Ratner, M. A. *J. Chem. Phys.* **1999**, *111*, 10069.

(44) Brudemann, J.; Lohbrandt, P.; Buck, U.; Buch, V. *J. Chem. Phys.* **2000**, *112*, 11038.

(45) Durup, J. Mechanisms of Collision-induced Dissociation of Fast Ions. in *Recent Developments in Mass Spectroscopy, Proceedings of the International Conference of Mass Spectroscopy*; Ogata, K., Hayakawa, T., Eds.; University Park Press: Baltimore, 1970; pp 921−934.

(46) Levine, R. D.; Bernstein, R. B. *Molecular Reaction Dynamics and Chemical Reactivity*; Oxford, New York, 1987.

(47) González Ureña, A. Influence of Translational Energy upon Reactive Scattering Cross Section: Neutral−neutral Collisions. In *Advances in Chemical Physics*; Prigogine, I., Rice, S. A., Eds.; John Wiley and Sons: New York, 1987; Vol. 66, pp 213−335.